Mode Perturbations of Microstrip Patch Antennas for Wideband, Multiband, and Mutual-Coupling Reduction Performances

Neng-Wu Liu*(1) and Lei Zhu(2)
(1) Xidian University, Xi'an, China; e-mail: nwliu@xidian.edu.cm; yb47448@umac.mo
(2) Macau University, Macau, China; e-mail: LeiZhu@um.edu.mo

Abstract

In this paper, we have studied the mode perturbation method of the planar patch antennas for the realization of wideband, multiband, and mutual coupling (MC) reduction performances. Compared with the traditional single-mode antenna, our proposed antennas based on the mode perturbation method have several advantages, such as single radiator, single layer, and high efficiency. Firstly, the working principle about how to perturbate the resonant frequencies of these radiative modes of the antennas is theoretically investigated. Secondly, several different topologies are extensively analyzed and discussed as examples in order to provide the physical insight into the working machine, aiming to prove their attractive performances in wireless communications.

1 Introduction

As is well known, the planar microstrip patch antennas (MPAs) have several advantages as compared to other non-planar antennas, such as small size, low profile, lightweight, simple structure, and easy conformability with circuits [1]. Unfortunately, the traditional MPAs based on the single mode suffer from narrow bandwidth, single band, or high mutual coupling (MC), which are all undesired in wireless communications.

In order to address these issues, the mode perturbation concept has been proposed and developed for the MPA during the past few years [2-6]. Meanwhile, it has received more and more attention in other worldwide teams. Firstly, the multi-mode operating in a large frequency range could be perturbated and reallocated in proximity to each other, leading to the wideband performance for the MPA in low-profile condition [2]. Secondly, the radiation pattern of the MPA working in different radiative modes could be perturbated and controlled. As a result, the MPA could successfully achieve the stable radiation pattern or stable gain as a function of multi-frequency bands [3]. Thirdly, the even- and odd-order modes of the single MPA could be perturbated and combined so as to bend the internal electric fields underneath the radiating patch, thus achieving the small MC under multi-mode, especially with the co-polarized and similar radiation patterns [4]. Additionally, by using the mode perturbation concept, the non-broadside beam of the MPA could be reshaped as the broadside-beam [5], the H-plane cross-polarization level of the MPA could be reduced [6], and so on.

In this paper, the mode perturbation method of the MPA will be revisited and used. Based on the HFSS simulation, the electric fields for its fundamental modes are theoretically studied. Then, the working machine about the multi-mode MPA is clearly explained based on the recent antenna examples via the shorting pins.

2 Mode Perturbation of Patch Antennas

In order to realize the wideband, multi-band, or MC reduction performances, the shorting pins, slots, and stubs are commonly used in order to perturbate the internal electric-field of these modes. As a result, we will take the TM_{01} and TM_{03} modes of the MPA as an example by using the shorting pins for theoretical investigation of the mode perturbation method.

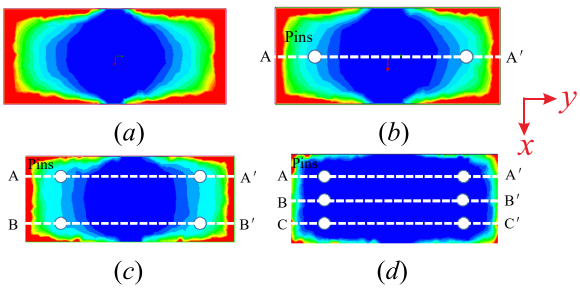

Figure 1. The internal electric-field perturbation of the MPA loaded with different pins at TM_{01} mode. (a) No pins. (b) Two pins. (c) Four pins. (d) Six pins.

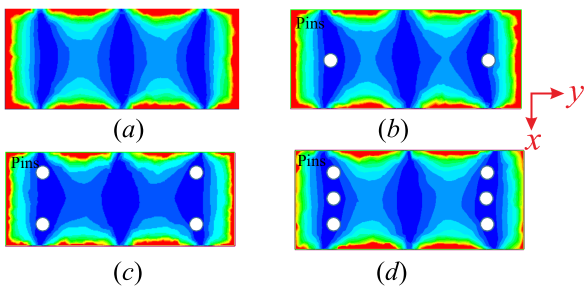

Figure 2. The internal electric-field perturbation of the MPA loaded with different pins at TM_{03} mode. (*a*) No pins. (*b*) Two pins. (*c*) Four pins. (*d*) Six pins.

Initially, Figs. 1 and 2 give the primary internal electric-field distribution of the MPA under different pins at TM_{01} and TM_{03} modes. With respect to the TM_{01} mode, its internal electric-field null is only formed around the center of the radiating patch in Fig. 1. With respect to the TM_{03} mode, its internal electric-field null is not only formed around the patch center, but also around the short distance from the patch edges in Fig. 2.

Then, Figs. 1(*b*) and 2(*b*) plot the internal electric-field distribution of the MPA loaded with two shorting pins. Compared to the primary results in Fig. 1(*a*), the maximum electric-field value has been reduced for its TM_{01} mode around the shorting pins, thus perturbating and reducing the resonant wavelength of this mode in this line AA′ . As a result, the resonant frequency of its TM_{01} mode could be increased. In contrast, the shorting pins are loaded around the minimum electric-field value of its TM_{03} mode in Fig. 2(*b*), which has a slight perturbation of the resonant frequency. Hence, the resonant frequency of the MPA at its TM_{03} mode keeps almost constant as compared to the results in Fig. 2(*a*).

After that, Figs. 1(*c*), 1(*d*), 2(*c*), and 2(*d*) illustrate the internal electric-field distribution of the single MPA loaded with four and six pins, respectively. It can be seen that the maximum electric-field value of TM_{01} mode could be further decreased down nearby these shorting pins. As such, the resonant wavelength of TM_{01} mode could be reduced around the line AA′ , BB′ and CC′ , which is more obviously as compared to the results in Fig. 1(*a*). In contrast, these additional pins are still installed around the minimum electric-field of its TM_{03} mode. Therefore, the resonant frequency of this mode gets slightly perturbated.

Apart from the shoring pins, the slots could be used to perturbate the minimum internal electric-field as the maximum counterpart. Thus, the slot is commonly cut on the radiating patch so as to increase the resonant wavelength as desired. Due to the page limitation, the electric-field variation of the single MPA under different slot lengths is not given herein.

3 Design Examples and Discussions

Based on the above mode perturbation principle, we would like to introduce the low-profile MPAs with improved functions in this section, such as bandwidth enhancement, multi-band realization, and MC reduction.

Firstly, the impedance bandwidth of the MPA is obviously enhanced by perturbating TM_{10} and TM_{30} modes as an example. Fig. 3 depicts the input resistance variation of the single MPA with and without these six pins. For the antenna without any pin perturbation, the frequency spacing between its TM_{10} and TM_{30} modes keeps a large value of 3, leading to the narrow bandwidth for the single-mode MPA. By loading six pins, the resonant frequency of its TM_{10} mode is obviously perturbated and increased, while keeping almost the constant for that of TM_{30} mode.

In order to verify the desired performance, the S-parameter comparison for the low-profile MPA with and without pins is illustrated in Fig. 4 The simulated and measured results have demonstrated that the mode perturbation method is successfully adopted to extend the operation bandwidth of the MPA, especially in low-profile condition. Similar to this working principle, the mode perturbation is also widely used in slot antennas, dipole antennas, dielectric resonant antennas for wide-bandwidth operation.

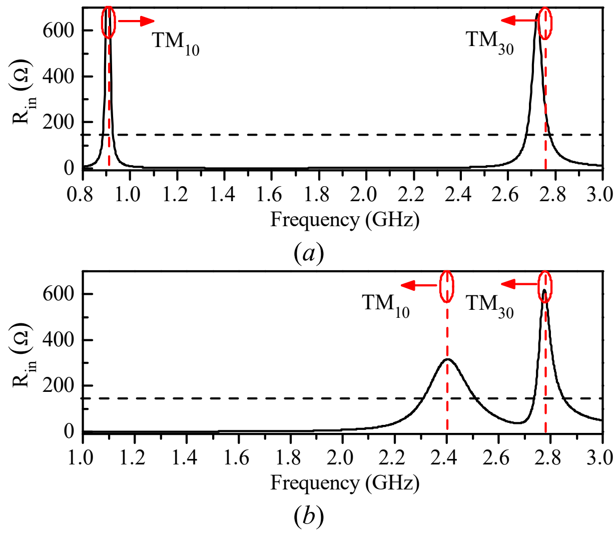

Figure 3. Input resistance of the MPA loaded with different number of shorting pins in [2]. (*a*) No pins. (*b*) Six pins.

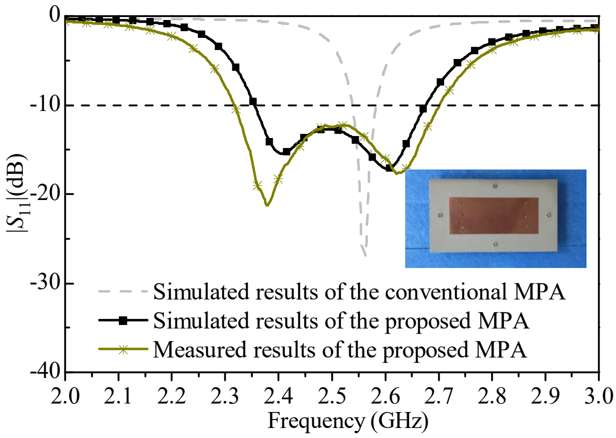

Figure 4. Simulated and measured $|S_{11}|$ of the proposed MPA in [2] loaded with six pins.

Secondly, the mode perturbation concept could be further adopted for multi-band antenna design. Fig. 5 plots the input resistance of the antenna under different pins and slots. For the traditional single MPA without any perturbation of pins and slots in Fig. 5(*a*), its TM_{10}, TM_{12}, and TM_{30} modes are independently resonating at 2.47, 5.6, and 7.18 GHz, respectively, which is not suitable for 2.4/5.2/5.8GHz WiFi communication. Most importantly, the radiation pattern of its higher TM_{12} mode suffers from the radiation null in broadside direction, and the radiation pattern of its higher TM_{30} mode keeps the large sidelobe level at E-plane. In order to address both of critical impedance and radiation issues, the shorted pins and slots are simultaneously loaded on the rectangular patch radiator, and the relevant results are given in Fig. 5(*b*). It observes that the input resistances of three modes are perturbated to around 2.4/5.2/5.8GHz. Particularly, the radiation patterns of its higher TM_{12} and TM_{30} modes are both reshaped into the broadside beam.

In order to verify the desired performance, the simulated and measured $|S_{11}|$ of the designed antenna are shown in Fig. 6, and good agreement between them exhibits that the antenna has achieved the impedance matching under three WiFi bands. Meanwhile, the radiation performance in Fig. 7 has proved that the stable peak gain nearby 7.5 dBi is successfully achieved via the mode perturbation method.

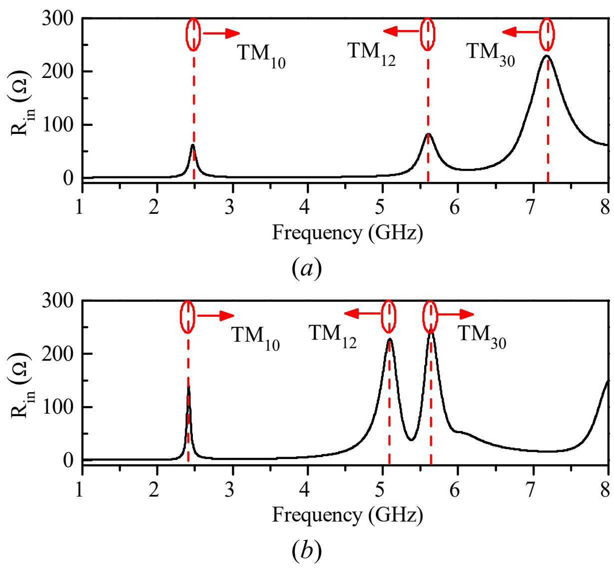

Figure 5. Input resistance of the MPA loaded with different number of shorting pins and slots in [3]. (*a*) No pins and slots. (*b*) Four pins and three slots.

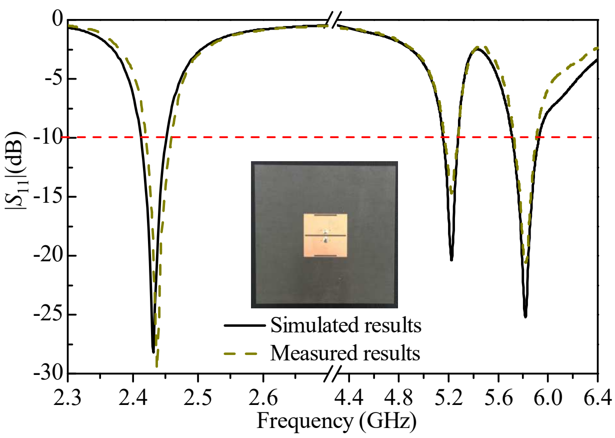

Figure 6. Simulated and measured $|S_{11}|$ of the proposed MPA in [3] loaded with four pins and three slots.

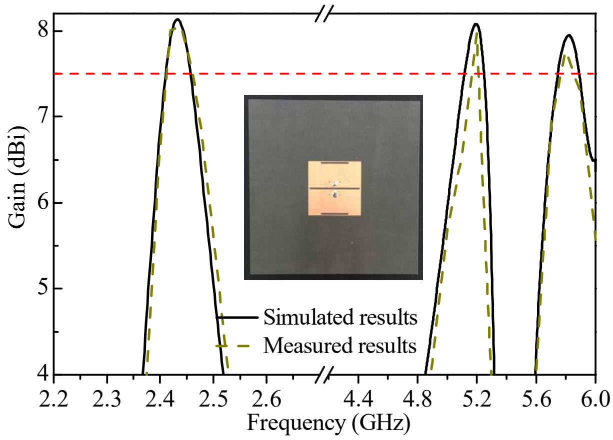

Figure 7. Simulated and measured gains of the proposed MPA in [3] loaded with four pins and three slots.

Thirdly, the mode perturbation concept could be adopted for mutual coupling reduction. Fig. 8 plots the input resistances of the two-port antennas with and without pins. For the traditional MPA without any pin perturbation, its mode 2 and mode 4 are independently excited at 3.14, and 5.87 GHz, respectively, which lead to the linear performance for their internal electric-field. By loading six pins around right side of the patch, the input resistance of mode 2 could turn up to around 5.75 GHz, and it keeps in proximity to that of mode 4. As such, the combined electric-field could be bent to around the unexcited feeding port as shown in Fig. 9. With this arrangement, the low MC performance could be realized.

In order to verify the desired performance, the S-parameter comparison for the low-profile MPAs with and without pins is illustrated in Fig. 10. The simulated and measured results have demonstrated that the mode perturbation method is indeed adopted to enhance the isolation between two ports from 3.5 dB to 17 dB under matched band. Noticing that, the similar radiation pattern and polarization are achieved at two ports independently.

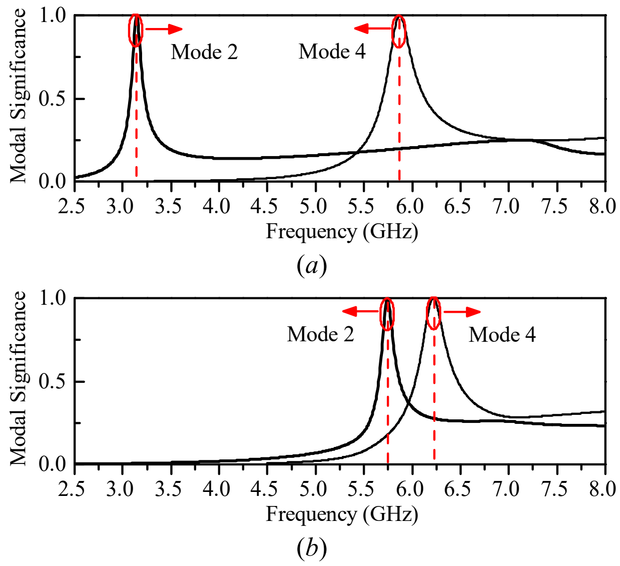

Figure 8. Input resistance of the two-port MPA loaded with different shorting pins in [4]. (*a*) No pins. (*b*) Six pins.

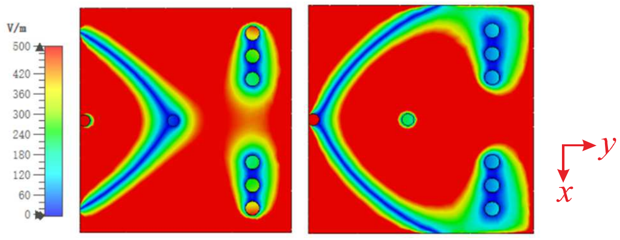

(*a*) (*b*)

Figure 9. Electric-field distributions of the MPA in [4] under different ports. (*a*) Left port excited. (*b*) Right port excited.

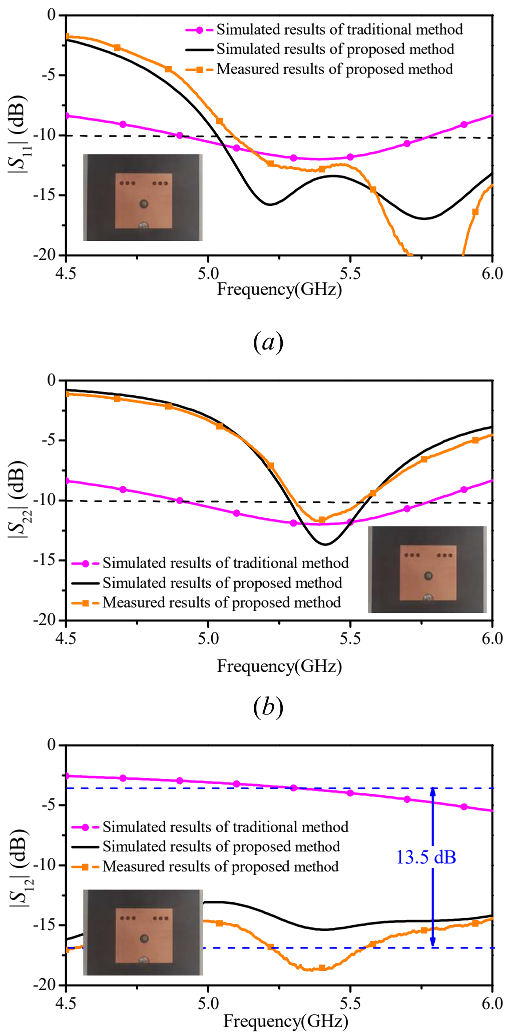

(*a*)

(*b*)

(*c*)

Figure 10. Simulated and measured S-parameter of the MPA in [4] loaded with six pins. (*a*) $|S_{11}|$. (*b*)$|S_{22}|$. (*c*) $|S_{12}|$

4 Conclusion

In this paper, we have illustrated the realization of a variety of advance performances for the low-profile MPAs by properly reallocating the resonant frequencies of several modes in a single patch radiator. Initially, the resonant frequencies of TM_{10} and TM_{30} modes could be perturbated and merged with each other, thus realizing the wide-bandwidth under multi-poles. Then, the TM_{10}, TM_{12}, TM_{30} modes could be shifted to three desired frequency points by loading the shorted pins and slots, thereby achieving the stable radiation gain in large frequency spacing. After that, the even-order mode 4 and odd-order mode 2 could be combined with each other so as to bend the electric-field distribution around the unexcited port. As such, the high isolation between these two ports could be successfully gained. Based on the above results, we believe that our proposed mode perturbation method has its attractive potential for wide application in various modern wireless communication systems.

Acknowledgements

This work was supported by the National Natural Science Foundation of China under General Program Grant s (61571468, 61801348, 61971475, and 62271364).

References

[1] Y. T. Lo, D. Solomon, and W. F. Richards, “Theory and Experiment on Microstrip Antennas,” *IEEE Transactions on Antennas and Propagation*, **27**, 2, Feb, 1979, pp. 137–145, doi: 10.1109/TAP.1979.1142057.

[2] N. -W. Liu, L. Zhu, W. -W. Choi, and X. Zhang, “A Low-Profile Aperture-Coupled Microstrip Antenna with Enhanced Bandwidth Under Dual Resonance,” *IEEE Transactions on Antennas and Propagation*, **65**, 3, March 2017, pp. 1055-1062, doi: 10.1109/TAP.2017.2657486.

[3] N. -W. Liu, X. -P. Chen, L. Zhu, X. Chen, G. Fu, and Y. Liu, “Low-profile triple-band microstrip antenna via sharing a single multi-mode patch resonator.” *IET Microwaves, Antennas and Propagation*, **13**, 10, 2019, pp. 1580-1585, doi:10.1049/iet-map.2018.5766.

[4] N. -W. Liu, Y. -D. Liang, L. Zhu, G. Fu, Y. Liu, and Y. Yun, “Electric-Field Null Bending of a Single Dual-Port Patch Antenna for Colinear Polarization Decoupling Using Characteristic Modes Analysis,” *IEEE Transactions on Antennas and Propagation*, **70**, 12, Dec. 2022, pp. 12247-12252, doi: 10.1109/TAP.2022.3206529.

[5] N. -W. Liu, L. Zhu, W. -W. Choi, and G. Fu, “A Low-Profile Wideband Aperture-Fed Microstrip Antenna with Improved Radiation Patterns,” *IEEE Transactions on Antennas and Propagation*, **67**, 1, Jan. 2019, pp. 562-567, doi: 10.1109/TAP.2018.2878099.

[6] N. -W. Liu, L. Zhu, Z. -X. Liu, Z. -Y. Zhang, G. Fu, and Y. Liu, “Cross-Polarization Reduction of a Shorted Patch Antenna with Broadside Radiation Using a Pair of Open-Ended Stubs,” *IEEE Transactions on Antennas and Propagation*, **68**, 1, Jan. 2020, pp. 13-20, doi: 10.1109/TAP.2019.2938742.